Atmospheric
Chemistry
and Physics
Discussions

Open Access

EGU

1 **Soil-atmosphere exchange of carbonyl sulfide in Mediterranean**

2 **citrus orchard**

3 Fulin Yang#, Rafat Qubaja, Fyodor Tatarinov, Rafael Stern, and Dan Yakir*

4

5 Earth and Planetary Sciences, Weizmann Institute of Science, Rehovot 76100, Israel

6

7 *#Present address*: College of Animal Sciences, Fujian Agriculture and Forestry

8 University, Fuzhou 350002, China

9

10 *Correspondence:* Dan Yakir; email: dan.yakir@weizmann.ac.il

11

Atmospheric
Chemistry
and Physics
Discussions

12      **Abstract:**

13          Carbonyl sulfide (COS) is used as a as a tracer of $CO_2$ exchange at the ecosystem

14      and larger scales. The robustness of this approach depends on knowledge of the soil

15      contribution to the ecosystem fluxes, which is uncertain at present. We assessed the

16      spatial and temporal variations of soil COS and $CO_2$ fluxes in the Mediterranean citrus

17      orchard combining surface flux chambers and soil concentration gradients. The spatial

18      heterogeneity in soil COS exchange indicated net uptake below and between trees of

19      up to -4.6 pmol m$^{-2}$ s$^{-1}$, and net emission in exposed soil between rows, of up to +2.6

20      pmol m$^{-2}$ s$^{-1}$, with weighted mean uptake values of -1.10 ± 0.10 pmol m$^{-2}$ s$^{-1}$. Soil

21      COS concentrations decreased with soil depth from atmospheric levels of ~450 to ~100

22      ppt at 20 cm depth, while $CO_2$ concentrations increased from ~400 to ~5000 ppm. COS

23      flux estimates from the soil concentration gradients were, on average, -1.02 ± 0.26 pmol

24      m$^{-2}$ s$^{-1}$, consistent with the chamber measurements. A soil COS flux algorithm driven

25      by soil moisture and temperature (5 cm depth) and distance from the nearest tree, could

26      explain 75% of variance in soil COS flux. Soil relative uptake, the normalized ratio of

27      COS to $CO_2$ fluxes was, on average -0.37 and showed a general exponential response

28      to soil temperature. The results indicated that soil COS fluxes at our study site were

29      dominated by uptake, with relatively small net fluxes compared to both soil respiration

30      and reported canopy COS fluxes. Such result should facilitate the application of COS

31      as a powerful tracer of ecosystem $CO_2$ exchange.

32

33      **Keywords:**

34      Carbonyl sulfide; COS; OCS; soil gas exchange; ecosystem gas exchange; tracer of

35      carbon fluxes.

## 1. Introduction

36

37      Carbonyl sulfide (COS) is a Sulphur-containing analogue of $CO_2$ that is taken up

38 by vegetation following a similar pathway to $CO_2$, ultimately hydrolyzed in an

39 irreversible reaction with carbonic anhydrase. It therefore holds great promise for

40 studies of photosynthetic $CO_2$ uptake (Asaf et al., 2013;Berry et al., 2013;Wehr et al.,

41 2017;Whelan et al., 2018). One of the difficulties in the application of COS as a tracer

42 for photosynthetic $CO_2$ uptake is the unknown non-leaf contributions the net ecosystem

43 COS flux. There are reports of significant soil fluxes, indicating both uptake and

44 emissions (Kesselmeier et al., 1999;Kuhn et al., 1999;Masaki et al., 2016;Seibt et al.,

45 2006;Yang et al., 2018;Yi et al., 2007). Although soil COS exchanges were often

46 considered small compared to plant uptake (e.g., Whelan et al., 2013;Yang et al., 2018),

47 this was not always the case. Significant soil COS emissions have been found in

48 wetlands and anoxic soils (Li et al., 2006;Whelan et al., 2013), and in senescing

49 agricultural fields and high temperatures (Liu et al., 2010;Maseyk et al., 2014), or under

50 drought conditions and in response to UV radiation (Kitz et al., 2017). Event for the

51 same soil, COS fluxes could show large variations and both uptake and emission with

52 sensitivities to soil moisture, and ambient COS concentrations (Bunk et al.,

53 2017;Kaisermann et al., 2018). These studies also assessed the response of COS

54 exchange to environmental controls, e.g. soil moisture and temperature and solar

55 radiation.

56      Soil COS exchange has often been measured by incubations in the lab (e.g., Bunk

57 et al., 2017;Kesselmeier et al., 1999;Liu et al., 2010;Van Diest and Kesselmeier, 2008),

58 and by static or dynamic chambers in the field (e.g., Berkelhammer et al., 2014;Kitz et

59 al., 2017;Sun et al., 2018;Yi et al., 2007;Mseyk et al., 2014), and using models (e.g.,

60 Ogée et al., 2016;Sun et al., 2015;Whelan et al., 2016). In spite of these efforts, more

61 field measurements of soil COS exchange are clearly needed as a basis for elucidating

62 underlying mechanism, as well as obtaining better quantitative record of the possible

63 range of soil COS fluxes under natural conditions. The objective of this study was to

64 apply dynamic chambers measurements, constrained by simultaneous soil gradient

65 method to assess the spatial and temporal variations soil COS and $CO_2$ fluxes in a citrus

Atmospheric
Chemistry
and Physics
Discussions

66    orchard ecosystem where contrasting soil microsite conditions occur.

67

68    **2.    Materials and methods**

69    **2.1  Field site**

70    The experiment was conducted in an orchard in Rehovot, Israel (31°54′ N, 34°49′

71    E, 50 m, asl) in 2015 and 2016. The orchard is a plantation of lemon trees (*Citrus*

72    *limonia Osbeck*), with 5 m distance between rows and 4 m between trees. Mean annual

73    air temperature at the site is 19.7 °C, and mean annual precipitation is 537 mm. Most

74    of the precipitation (82%) falls in November to February with no rain during June to

75    October. A trickle irrigation system was used from May to September with the standard

76    irrigation plan of the orchard management. The soil in the area is red sandy soil with an

77    average bulk density of 1.6 kg m$^{-3}$ (Singer, 2007).

78

79    **2.2  Quantum cascade laser measurements**

80    We used the commercially available quantum cascade laser (QCL) system

81    (Aerodyne Research, Billerica, MA) with tunable laser absorption spectrometer (Model:

82    QC-TILDAS-CS) to measure COS, $CO_2$, and water vapor concentrations

83    simultaneously. The device was installed in a mobile lab, described in the Asaf et al.

84    (2013). COS is detected at 2050.40 cm$^{-1}$ and $CO_2$ at 2050.57 cm$^{-1}$ at a rate of 1 Hz.

85    The instrument was calibrated using working reference compressed air tank that was

86    used for inter-comparison with the NOAA GMD lab (Boulder CO).

87

88    **2.3  Soil chamber flux measurements**

89    Custom-made stainless-steel cylindrical chamber of 177 cm$^2$ directly inserted into

90    the soil (~5 cm) was used, as previously described (Berkelhammer et al., 2014;Yang et

91    al., 2018). The chamber air and ambient air flows were pumped to the QCL analyzer

92    through two 3/8-inch diameter Decabon tubing. Flow rate was maintained at 1.2 L min$^-$

93    $^1$ and repeatedly cycled with 1 min instrument background (using $N_2$ zero gas), 9 min

94    ambient air flow, and 10 min chamber air sample. Three different soil sites were used

95    with distance of 3.20, 2.00 and 0.25 m away from a tree trunk, that represented sampling

96    sites between rows (BR), between trees (BT) and under tree (UT). Each sampling site

97    was measured continuously for 24 hours and cycled between sites for the duration of

98    the campaign. Four measurement campaigns were carried out during 5th~9th August

99    2015; 25th~28th December 2015; 5th~9th May 2016; 28th~31th July 2016.

100        Gas exchange rates, $F_c$, were calculated according to:

101 $$F_c = \frac{Q}{A} \times \left( \Delta C_{sample} - \Delta C_{blank} \right) \qquad (1)$$

102    where $Q$ is the chamber flush rate in mol s$^{-1}$; $A$ is the enclosed soil surface in m$^2$; $\Delta C$ is

103    the gas concentrations difference between chamber air and ambient air in pmol mol$^{-1}$

104    for COS and μmol mol$^{-1}$ for $CO_2$ under sampling, and blank reference treatments (using

105    the same chamber placed above a sheet of aluminum foil before and after measurement

106    at each site. Hereafter, the soil fluxes are reported in pmol m$^{-2}$ s$^{-1}$ and μmol m$^{-2}$ s$^{-1}$ for

107    COS and $CO_2$, respectively. Soil relative uptake (SRU) is used to characterize the

108    relationship between soil $CO_2$ and COS fluxes, was estimated from the normalized ratio

109    of COS to $CO_2$ and uptake (negative values), or emission (positive values) fluxes

110    (Berkelhammer et al., 2014):

111 $$SRU = \frac{F_{COS_{soil}}}{[COS]} \bigg/ \frac{F_{CO_{2soil}}}{[CO_2]} \qquad (2)$$

112

113    **2.4  Soil concentration profile measurements**

114        Four campaigns of soil concentration profile measurements were carried out

115    during 1st~2nd March; 20th~26th April; 10th May; 22nd~28th June of 2016. The trace

116    gas at five soil depths of 0, 2.5, 5.0, 10, 20 cm was sampled at each of the three

117    microsites, BR, BT and UT.

118        Four Decabon tubing were inserted into the soil at the different depth and connect

119    directly to the QCL. At least one day after insertion, soil air was sampled with flow rate

120    of 400 ml min$^{-1}$, in cycles of 1 min instrument background-3 min surface air (depth 0)-

121    5 min sampling of a depth point in the profile-1 min surface air. Each cycle was,

122    therefore, 10 min. Five complete sets of cycles including the four soil depths and

123    surface air were repeated for each site.

124     Assuming that in the selected measurement sites, soil trace gas is only

125     transported by diffusion, soil COS and $CO_2$ fluxes estimated based on the Fick's first

126     law according to:

127
$$F = -D_s \frac{dC}{dz} \qquad (3)$$

128     where $F$ is the upward or downward gas flux (pmol m$^{-2}$ s$^{-1}$ for COS and μmol m$^{-2}$ s$^{-1}$

129     for $CO_2$); $D_s$ is the effective gas diffusion coefficient of the relevant gas species in the

130     soil (m$^2$ s$^{-1}$); $C$ the trace gas concentration (mixing ratio, converted from the measured

131     mole fractions); $z$ is the soil depth (m).

132     The Penman (1940) function was used to describe the soil diffusion coefficient

133     ($D_s$) as in Kapiluto et al. (2007):

134
$$D_s = D_a \left( \theta_s - \theta \right) \sqrt{\frac{T_s + 273.15}{298.15}} \qquad (4)$$

135     where $\theta_s$ is the soil saturation water content and $\theta$ is the measured soil volumetric water

136     content. $D_a$ is the trace gas diffusion coefficient in free air, which varied with

137     temperature and pressure, given by

138
$$D_a = D_{a0} \left( \frac{T + 273.15}{293.15} \right)^{1.75} \left( \frac{P}{101.3} \right) \qquad (5)$$

139     where $D_{a0}$ is a reference value of trace gas diffusion coefficient at 293.15 K and 101.3

140     kPa, given as $1.24 \times 10^{-5}$ m$^{-2}$ s$^{-1}$ for COS (Seibt et al., 2010) and $1.47 \times 10^{-5}$ m$^{-2}$ s$^{-1}$

141     for $CO_2$ (Jones, 1992); $T$ is temperature (ºC), and $P$ is air pressure (kPa).

142

143     **3. Results**

144     **3.1 Variations in soil COS flux**

145     Soil COS fluxes showed significant heterogeneity at both the spatial (microsites)

146     and temporal (seasonal), as well as interactions between microsite and season (Figure

147     1, Table 1). Overall, the hourly soil COS flux varied from -4.6 to +2.6 pmol m$^{-2}$ s$^{-1}$,

148     with mean value of -1.10 ± 0.10 pmol m$^{-2}$ s$^{-1}$. On the spatial scale, the COS fluxes

149     showed systematically uptake under trees (UT), moderate uptake and some emissions

150     between trees (BT) and relatively more emission in the exposed area between rows

Atmospheric
Chemistry
and Physics
Discussions

151    (BR), with diurnal mean values across seasons of -3.00 ± 0.10, -0.43 ± 0.13 and 0.13 ±

152    0.11 pmol m$^{-2}$ s$^{-1}$, respectively.

153         On the diurnal time-scale, soil COS flux were generally higher in the afternoon

154    (peaking around 15:00~16:00 hours), declining at night and early morning (Fig. 1). On

155    the seasonal time scale, soil COS fluxes showed both changes in rates and shifts from

156    net uptake to net emission, with interactions between site and season (Table 1). In the

157    UT sites where only COS uptake was observed, the highest rates were observed in

158    winter and peak summer (December and Auguest) with diurnal mean rates of nearly 4

159    pmol m$^{-2}$ s$^{-1}$, and more moderate uptake rates, around 2 pmol m$^{-2}$ s$^{-1}$, in spring and early

160    summer (May and July; Fig. 1). In the BT sites, significant COS uptake of ~-2.5 pmol

161    m$^{-2}$ s$^{-1}$ was observed in winter, but net fluxes were near zero in other times, with some

162    afternoon emission in summer. In the exposed BR sites, minor uptake (less than 1 pmol

163    m$^{-2}$ s$^{-1}$) was observed in spring and early summer, but consistent emission in peak

164    summer, with diurnal mean values of nearly 2 pmol m$^{-2}$ s$^{-1}$.

165

166    **3.2 Effects of moisture and temperature**

167         During the hot summer (August 2015 and July 2016), differences in microsite soil

168    water content ($\theta$) were most distinct, with $\theta$ of nearly 30% in the UT sites (associated

169    with drip irrigation), but ~19% and ~12% in the BT and BR sites. Correspondingly, the

170    UT sites had significant COS uptake of about -3 pmol m$^{-2}$ s$^{-1}$ while the other sites

171    showed emission of about +1 pmol m$^{-2}$ s$^{-1}$ (Table 1). In winter (December), $\theta$ in the

172    three sites was similar ~25% and all sites showed soil COS uptake, but with clear

173    gradient of -3.9, -2.5 and -0.7 pmol m$^{-2}$ s$^{-1}$ in the UT, BT and BR sites, respectively

174    (Table 1). On average, soil COS fluxes showed non-linear increase in uptake with

175    increasing $\theta$, but it seems that this response may saturate at about $\theta$ of 25% and uptake

176    rates of ~3.9 pmol m$^{-2}$ s$^{-1}$ (Fig. 2). The best fit line to the data presented in Fig. 2 also

177    indicate that in dry soil with $\theta$<15% soil COS emission can be expected.

178         The response of soil COS fluxes to soil temperature varied among the three

179    measurement sites (Fig. 3). The BT and BR sites showed a near linear response with a

180    shift from uptake to emisson around 25 °C. In the shaded and moist UT site, COS uptake

Atmospheric
Chemistry
and Physics
Discussions

181    was always significant ranging between -4 to -1 pmol m$^{-1}$ s$^{-1}$ with relatively low

182    temperature sensitivity, and with lowest mean uptake rates around 20 °C.

183        Pearson product-moment correlation analysis results showed that hourly soil COS

184    flux was significantly related to soil moisture and temperature (at the 0.001 level), and

185    the soil moisture had a stronger environmental controls on the soil COS flux ($r$=-0.77),

186    compared with soil temperature ($r$=+0.45).

187        Comprehensive assessment of the effects of soil moisture ($\theta$), temperature ($Ts$) and

188    distance away from tree trunk ($d$) , hourly soil COS flux ($F_{COS}$) could be fitted to a three

189    parameters exponential model, which could explain 75% of the variation in soil COS

190    flux (Eq. 6).

191        $$F_{COS} = 8.91\exp(0.01Ts - 0.01\theta + 0.09d - 0.33) - 8.86, \; R^2 = 0.75 \quad (6)$$

192

193    **3.3 COS flux estimates from soil concentration gradients**

194        The average soil concentration gradient of COS and $CO_2$ for the four campaigns

195    is shown in Fig. 4. COS concentrations decreased with soil depth, with the opposite

196    trend for $CO_2$, consistent with the results reported above of soil surface COS uptake

197    and $CO_2$ emission at our orchard site. COS concentrations at depth of 2.5 cm was on

198    average 314 ppt, and about one-third lower than the mean surface, ambient, value of

199    460 ppt. The lowest COS concentration at depth of 20 cm (166 ppt) was almost one-

200    third of that at the soil surface. An exponential and a linear equations provided

201    reasonable fit to the changes in soil COS and $CO_2$ concentrations, respectively, as a

202    function of depth ($z_{soil}$):

203
$$[COS] = 283.5\exp\left(-0.2z_{soil}\right) + 169.9, \; R^2 = 0.99$$
$$[CO_2] = 122.2z_{soil} + 558.5, \; R^2 = 0.99$$
$$(7)$$

204        In terms of individual site and campaign, all profiles except for BR in summer

205    (June) showed the general trend of decreasing [COS] and increasing [$CO_2$] with depth,

206    with the steepest gradient at the top 5 cm (Fig. 4). In the BR microsite in summer, $CO_2$

207    profile was shallow, consistent with the low respiration (see July BR in Table 1). But a

208    decrease in COS concentration toward the surface, with surface value lower than the

Atmospheric
Chemistry
and Physics
Discussions

209    next two soil depth points (Fig. 5J), was consistent with COS emission at that time (July

210    BR in Table 1).

211        As noted above, the profile data generally exhibited the steepest gradient at the top

212    few cm of the soil, indicating that the dominating COS sink (and likely also the $CO_2$

213    source) was located at shallow depth. We therefore used the gas concentration

214    difference at two shallowest depths ($z_1 = 0$ and $z_2 = 2.5$ cm) to provide an approximation

215    of the fluxes to and from the soil, to constrain the more extensive chamber

216    measurements. The COS diffusion coefficient, $D_s$, was estimated for each campaigns

217    (see Methods), indicating low $D_s$ value in the UT site in June and July ($D_s = 2.55$ mm$^2$

218    s$^{-1}$), associated with the drip irrigation and the high soil water content, and high values

219    in the dryer soils ($D_s = 5.57$ mm$^2$ s$^{-1}$), with an average COS diffusion coefficient of 4.40

220    $\pm$ 0.29 mm$^2$ s$^{-1}$. The soil COS flux estimates using the gradient method is reported in

221    Table 2. COS flux varied between -2.10 to +1.55 pmol m$^{-2}$ s$^{-1}$ with a mean value of -

222    1.0 $\pm$ 0.26 pmol m$^{-2}$ s$^{-1}$ during the measurement periods, consistent with the mean value

223    of -1.10 $\pm$ 0.10 pmol m$^{-2}$ s$^{-1}$ reported above for the chamber measurements. Also in

224    agreement with the chamber measurements, fluxes at UT and BT always showed COS

225    uptake, with generally higher values in spring (March) than in summer (May-June),

226    while the BR data indicated change from uptake in spring (March-April, with -1.3 to -

227    1.6 pmol m$^{-2}$ s$^{-1}$) to emission in June (+1.6 pmol m$^{-2}$ s$^{-1}$).

228

229    **3.4 Soil relative uptake**

230        Soil was always a source of $CO_2$ due respiration (combined autotrophic and

231    heterotrophic respiration). Soil $CO_2$ flux rates varied both spatially and temporally in

232    similar patterns to those of COS, and with overall range of 0.3 to 14.6    mol m$^{-2}$ s$^{-1}$

233    (Table 1). The highest soil respiration values were observed in the UT sites in summer

234    (July, August; Table 1), with intermediate (1~3    mol m$^{-2}$ s$^{-1}$) and low values (< 1

235    mol m$^{-2}$ s$^{-1}$) in the BT and BR sites, respectively. Generally, soil COS exchange

236    varied from release to increasing uptake with increasing $CO_2$ production in a non-linear

237    way (Fig. 6a). The normalized ratio of COS to $CO_2$ fluxes (SRU; Eq. 2) varied from -

238    1.92 to +1.85 with an average value of -0.37 $\pm$ 0.31, with negative values indicating

239    COS uptake linked to $CO_2$ emission. SRU values showed response to both soil

240    temperature (Fig. 6b) and soil moisture (Fig. 6c), although with relatively low $R^2$ values.

241    Respiration increased with temperature while COS uptake declined and at temperature

242    above about 25 °C SRU turned positive when both COS and $CO_2$ are emitted from the

243    soil. SRU exhibited inverse relationships with soil moisture, with positive values in dry

244    soil and increasingly negative values with increasing soil moisture (Fig. 6c). Based on

245    its combined temperature ($Ts$) and moisture ($\theta$) response, SRU could be forecasted by

246    the following algorithm, which explained 67% of the observed variations (Eq. 8):

247    $$SRU = 0.01\exp(0.17Ts) - 0.02\theta - 1.00, \ R^2 = 0.67 \qquad (8)$$

248    ANOVA analysis results indicated that SRU was not significantly different among

249    the three observation microsites (BR, BT, and UT; $P > 0.05$). Between the seasonal

250    campaigns, however, SRU values peaked in summer ($0.53 \pm 0.66$) with highest

251    averaged soil temperature (29 °C) and was significantly higher than winter SRU (-1.44

252    $\pm$ 0.59) when soil temperature was lowest (11 °C; $P < 0.05$), and with no significant

253    difference in SRU among the other campaigns ($P > 0.05$).

254

255    **4. Discussions**

256    **4.1 Heterogeneity in soil COS exchange**

257    The observed soil-atmosphere COS exchange rates observed in this study (both

258    mean and range; Fig. 1, Table 1) are consistent with values reported in a range of other

259    ecosystems (-1.4 to -4.9 pmol m$^{-2}$ s$^{-1}$; Steinbacher et al., 2004;Kitz et al., 2017;White

260    et al., 2010;Berkelhammer et al., 2014), but lower than -11.0 to -11.8 pmol m$^{-2}$ s$^{-1}$ in a

261    riparian and subtropical forests (Berkelhammer et al., 2014;Yi et al., 2007). Soil COS

262    emissions were also observed in summer and spring campaigns, with maximal COS

263    emission consistent with the values of +1.8 to +2.6 pmol m$^{-2}$ s$^{-1}$ observed in a riparian

264    and alpine forests (Berkelhammer et al., 2014), but significantly lower than reported in

265    the senescing agricultural ecosystem (~30 pmol m$^{-2}$s$^{-1}$; Maseyk et al., 2014).

266    The observed range in the soil-atmosphere exchange fluxes reflected significant

267    heterogeneity on both the spatial and the temporal scales. The spatial scale

Atmospheric
Chemistry
and Physics
Discussions

268    heterogeneity clearly reflected the contrasting microsite conditions with lower

269    temperatures and higher moisture under the trees (UT sites), compared to the higher

270    temperatures and lower moisture in exposed soil between rows (BR sites), with

271    intermediate, partially shaded, conditions between trees (BT sites). Indeed, a large

272    fraction of the variations in the COS flux (~75%) could be explained by a simple

273    algorithm as a function of these two variables, temperature and moisture. Note that

274    while temperature and $\theta$ co-varied in general, with high temperatures associated with

275    drier soil, under the wet UT conditions, sensitivity to temperature was significantly

276    reduced. In the dry soil conditions, emission was associated with high temperature, and

277    in the BR sites also with high solar radiation. However, all measurements we made in

278    dark chamber and could not involve photochemical production (Kitz et al., 2017).

279    Apparently even under dark conditions, high temperature can induced high emission

280    rates, as also noted when the thermal insolation on the soil chamber in the BR site was

281    incidentally removed and a large spike in temperature (52 °C) and emission of 11.4

282    pmol m$^{-2}$ s$^{-1}$ was observed.

283        Temporal variations were observed both on the daily and seasonal time scales.

284    Diurnal changes were, however, minor compared to the changes from winter to summer

285    in all microsites. Shifts from uptake to emission were observed essentially only on the

286    seasonal time scale (Fig. 1). This likely reflected the dominance of soil moisture on the

287    COS flux rates. This is because $\theta$ did not change significantly on the daily scale, while

288    it changed significantly on across seasons (between 10.0 and 35.5% overall).

289    Temperatures did change over the daily cycle (e.g. 26.0 to 42.4 °C in the BR site during

290    summer), although such changes are still smaller compared with the seasonal changes

291    in soil temperature (e.g. 10.5 to 31.8 °C in the BR site). A dominant role of soil moisture

292    in explaining the variations in COS uptake is consistent with the results of Van Diest

293    and Kesselmeier (2008), but not with the negligible $\theta$ effects in grassland under

294    simulated drought (Kitz et al., 2017). Soil moisture can influence soil COS exchanges

295    by influencing CA enzymatic activity (Davidson and Janssens, 2006;Seibt et al., 2006),

296    changing soil gas diffusion rates (Ogée et al., 2016;Sun et al., 2015), and vegetation

297    root distribution and the effects of CA activity within plant roots (Seibt et al.,

Atmospheric
Chemistry
and Physics
Discussions

298    2006;Viktor and Cramer, 2005;Whelan and Rhew, 2015). In this study, most of the roots

299    were distributed around the restricted trees' drip irrigation zone at UT sites, and was

300    sparse in the dryer areas, such as BR and BT sites (un-quantified observations).

301        At least part of the variations in soil COS fluxes could also reflect the differential

302    effects of environmental conditions on COS uptake and production process (Ogée et al.,

303    2016). COS uptake is thought to be related to carbonic anhydrase activity in soil

304    microorganisms (Piazzetta et al., 2015), such as Bacteria (Kamezaki et al., 2016;Kato

305    et al., 2008), or fungi (Bunk et al., 2017;Li et al., 2010;Masaki et al., 2016). Solubility

306    in soil water (with COS solubility of 0.8 ml ml$^{-1}$; Svoronos and Bruno, 2002) could also

307    be significant, especially in the UT microsites, influenced by the drip irrigation from

308    May to September that could involve water percolation to deeper soil layers. The drivers

309    of soil COS production are still unclear. COS could be produced by chemical processes

310    in the lab (Ferm, 1957), but can also be produced by biotic process in soils such as by

311    hydrolysis of metallic thiocyanates (Katayama et al., 1992) with thiocyanate hydrolase

312    (Conrad, 1996;Svoronos and Bruno, 2002) and hydrolysis of $CS_2$ (Cox et al.,

313    2013;Smith and Kelly, 1988). Fungi are also reported to be the source of COS (Masaki

314    et al., 2016). Additionally, abiotic thermal degradation of organic matter leading to COS

315    production maybe supported by the temperature sensitivity of COS emission in the BR

316    microsite where biotic processes can be expected to be minimized. Similar high

317    temperature-dependent soil COS emissions were reported in midlatitude forest

318    (Commane et al., 2015) and agricultural field (Maseyk et al., 2014). Lab incubation

319    results also indicated soil thermo production of COS with increasing temperature (Liu

320    et al., 2010;Whelan et al., 2016;Whelan and Rhew, 2015). Photochemical production

321    of soil COS was also proposed (Sun et al., 2015;Whelan and Rhew, 2015), and assumed

322    to be driven by ultraviolet fraction of incoming solar radiation (Kitz et al., 2017). Note,

323    however, that all measurements in the present study were made in the dark. In addition,

324    the chemical reaction of CO and $MgSO_4$ under heating could also produce COS (Ferm,

325    1957). Note that $MgSO_4$ has been reported in our study soil (Singer, 2007), and we

326    observed relatively high CO concentration in our field site.

327

### 4.2 Soil relative uptake

328  

329 For COS application as a tracer of ecosystem $CO_2$ exchange quantifying the

330 relationships between COS and $CO_2$ fluxes is important. This is done by assessing the

331 'relative uptake' (RU) of the COS/$CO_2$ flux rate ratio, normalized by the ambient

332 atmospheric concentrations (that differ for the two gases by a factor of about $10^6$), as

333 done at the leaf, (LRU) or ecosystem (ERU; e,g, Asaf et al., 2013). It was similarly

334 applied to soil as SRU (Eq. 2; Berkelhammer et al., 2014). We use SRU values also to

335 assess the relative importance of the soil COS flux compared with the canopy.

336 On average, the absolute value of SRU at our site was smaller than reported for

337 riparian or pine forests (0.37 vs 0.76 and 1.08; Berkelhammer et al., 2014). This may

338 reflect the contribution of COS emissions at BR and BT in summer, that were not

339 observed in the forest study. Overall, the mean SRU values observed here indicated that

340 the soil COS uptake flux was proportionally less than 40% of the soil respiration flux.

341 In contrast with the canopy fluxes where the COS uptake flux is, proportionally, nearly

342 twice as large as the $CO_2$ assimilation flux (LRU~1.7; see review of Whelan et al.,

343 2018). In contrast to leaves with robust LRU value that tend toward a constant, SRU at

344 our site varied between -1.92 and +1.85. However, this range was observed only in the

345 dryer and exposed BR sites, while in the shaded and moist UT sites, it was much

346 narrower, -0.13 to -0.79. Furthermore, it seems that the high SRU values (both positive

347 and negative) represented conditions where the actual fluxes were small (COS uptake

348 was on average -3.0 in the UT but only 0.1 pmol m$^{-2}$ s$^{-1}$ in the BR sites. It seems that

349 the large SRU values in the BR microsites, were also associated with low soil

350 respiration, 0.5 mol m$^{-2}$ s$^{-1}$ in BR sites, compared to 10 mmol m$^{-2}$ s$^{-1}$ in the UT sites.

351 It is therefore possible that the low SRU values are the more significant for ecosystem

352 scale studies and indicate a much smaller contribution to overall ecosystem fluxes than

353 that of the canopy (SRU~0.4 vs LRU~1.7).

354 Differential effects of changing environmental conditions on production and

355 uptake processes were reflected in relatively large spatial and temporal heterogeneity

356 observed in the soil COS exchange at our site. However, the contrasting effects of

357 production and emission may explain both the sharp increase in SRU values at high

Atmospheric
Chemistry
and Physics
Discussions

358    temperatures as the effects of production counteract uptake (Fig. 6b), and the much

359    lower sensitivity to temperature of COS flux compared to that of $CO_2$ (Fig. 6a). Such

360    contrasting consumption/production effects may, in fact, reduce the magnitude of the

361    net flux of soil COS, and may explain the relatively narrow range of SRU values.

362

**4.3 Soil COS profiles**

364        Complementing our chamber measurements with soil profile measurements of

365    COS and $CO_2$ concentrations provided constrain on the relatively new surface soil COS

366    measurements and provided additional information on the possible location of the

367    source/sink in the soil. Using the near surface gradient yielded flux estimates

368    comparable to chamber measurements, providing a useful and rare quantitative

369    validation. For example, in May, the chamber and profile measurements were made at

370    about the same time (5th~9th May for chamber and 10th May for profile) and the

371    differences between chamber (all microsites) and gradient flux estimates, was

372    negligible (~0.2-0.6 pmol m$^{-2}$ s$^{-1}$). However, the profile results indicated in addition that

373    the sink/source activities concentrated at top soil layers, probably at around 5 cm depth,

374    as reflected in the minimum or maximum in gas concentrations (indicating also the need

375    for high vertical resolution in employing the profile approach). The variable profiles

376    observed below these points must reflect temporal dynamics in the sink/source

377    activities across the profile. The near surface peak activity makes it particularly

378    sensitive to variations in temperature and moisture, as indeed observed (Figs. 2, 3). Low

379    COS concentration in the lower parts of the profile may result from continuous removal

380    of soil COS and may indicate distribution of CA activity beyond the litter layer and the

381    soil surface (Seibt et al., 2006). COS production, however, seems to occur only near the

382    soil surface with no indication for production in deeper layer, consistent with its high

383    temperature sensitivity, and possibly also radiation (e.g. Kitz et al., 2017).

384        Note that the gradient method based on Fick's diffusion law have its own

385    limitations (Kowalski and Sánchezcañete, 2010;Sánchez-Cañete et al., 2017;Bekele et

386    al., 2007). However, it is simple low-cost approach and can help diagnose the

387    magnitude of soil fluxes, which can also help in identifying below ground processes

Atmospheric
Chemistry
and Physics
Discussions

388 and their locations.

389

390 **5. Conclusions**

391     Our detail analysis of the spatial and temporal variations in soil-atmosphere

392 exchange of COS provided new information on a key uncertainty in the application of

393 ecosystem COS flux to assess productivity. Furthermore, we provide constraint, and

394 validation of the close chamber measurements that are generally in use, by the

395 additional gradient approach. Our results show that both microsites and seasonal

396 variations in COS fluxes were related to soil moisture, temperature, and the distance

397 from the tree (likely reflecting root distribution), but we suggest that soil moisture is

398 the predominant environmental control over soil COS exchanges at our site. A simple

399 algorithm was sufficient to forecast most of the variations in soil COS flux supporting

400 its incorporated into ecosystem scale applications, as we recently demonstrated in a

401 parallel study at the same site (Yang et al., 2018).

402     Clearly, uncertainties are still associated with soil processes involving COS, the

403 differential effects of soil moisture, temperature, and communities of microorganisms

404 and are likely to contribute to both the spatial and temporal variations in soil net COS

405 exchange and require further research.

406

407 **Author contributions:**

408     DY designed the study; FY, RQ, FT, RS and DY performed the experiments. FY

409 and FT analysed the data. DY and FY wrote the paper with discussions and

410 contributions to interpretations of the results from all co-authors.

411

Atmospheric
Chemistry
and Physics
Discussions

418  **References**

419  Asaf, D., Rotenberg, E., Tatarinov, F., Dicken, U., Montzka, S. A., and Yakir, D.:

420      Ecosystem photosynthesis inferred from measurements of carbonyl sulphide flux,

421      Nat. Geosci., 6, 186-190, 2013.

422  Bekele, A., Kellman, L., and Beltrami, H.: Soil Profile $CO_2$ concentrations in forested

423      and clear cut sites in Nova Scotia, Canada, Forest. Ecol. Manag., 242, 587-597,

424      2007.

425  Berkelhammer, M., Asaf, D., Still, C., Montzka, S., Noone, D., Gupta, M., Provencal,

426      R., Chen, H., and Yakir, D.: Constraining surface carbon fluxes using in situ

427      measurements of carbonyl sulfide and carbon dioxide, Global Biogeochem. Cy.,

428      28, 161-179, 2014.

429  Berry, J., Wolf, A., Campbell, J. E., Baker, I., Blake, N., Blake, D., Denning, A. S.,

430      Kawa, S. R., Montzka, S. A., and Seibt, U.: A coupled model of the global cycles

431      of carbonyl sulfide and $CO_2$: A possible new window on the carbon cycle, J.

432      Geophys. Res.:Biogeo., 118, 842-852, 2013.

433  Bunk, R., Behrendt, T., Yi, Z., Andreae, M. O., and Kesselmeier, J.: Exchange of

434      carbonyl sulfide (OCS) between soils and atmosphere under various $CO_2$

435      concentrations, J. Geophys. Res.:Biogeo., 122, 1343-1358, 2017.

436  Commane, R., Meredith, L. K., Baker, I. T., Berry, J. A., Munger, J. W., Montzka, S. A.,

437      Templer, P. H., Juice, S. M., Zahniser, M. S., and Wofsy, S. C.: Seasonal fluxes of

438      carbonyl sulfide in a midlatitude forest, P. Natl. Acad. Sci. U.S.A., 112, 14162-

439      14167, 2015.

440  Conrad, R.: Soil microorganisms as controllers of atmospheric trace gases ($H_2$, CO,

441      $CH_4$, OCS, $N_2O$, and NO), Microbiol. Rev., 60, 609-640, 1996.

442  Cox, S. F., McKinley, J. D., Ferguson, A. S., O'Sullivan, G., and Kalin, R. M.:

443      Degradation of carbon disulphide (CS2) in soils and groundwater from a $CS_2$-

444      contaminated site, Environ. Earth Sci., 68, 1935-1944, 2013.

445  Davidson, E. A., and Janssens, I. A.: Temperature sensitivity of soil carbon

446      decomposition and feedbacks to climate change, Nature, 440, 165-173, 2006.

447  Ferm, R. J.: The chemistry of carbonyl sulfide, Chemical Reviews, 57, 621-640, 1957.

448    Jones H G . Plants and Microclimate: A Quantitative Approach to Environmental Plant

449        Physiology, Cambridge University Press, 1983.

450    Kaisermann, A., Ogée, J., Sauze, J., Wohl, S., Jones, S. P., Gutierrez, A., and Wingate,

451        L.: Disentangling the rates of carbonyl sulfide (COS) production and consumption

452        and their dependency on soil properties across biomes and land use types, Atmos.

453        Chem. Phys., 18, 9425-9440, 2018.

454    Kamezaki, K., Hattori, S., Ogawa, T., Toyoda, S., Kato, H., Katayama, Y., and Yoshida,

455        N.: Sulfur Isotopic Fractionation of Carbonyl Sulfide during Degradation by Soil

456        Bacteria, Environ. Sci. Technol., 50, 3537-3544, 2016.

457    Kapiluto, Y., Dan, Y., Tans, P., and Berkowitz, B.: Experimental and numerical studies

458        of the $^{18}O$ exchange between $CO_2$ and water in the atmosphere–soil invasion flux,

459        Geochim. Cosmochim. Ac., 71, 2657-2671, 2007.

460    Katayama, Y., Narahara, Y., Inoue, Y., Amano, F., Kanagawa, T., and Kuraishi, H.: A

461        thiocyanate hydrolase of Thiobacillus thioparus. A novel enzyme catalyzing the

462        formation of carbonyl sulfide from thiocyanate, J. Biol. Chem., 267, 9170-9175,

463        1992.

464    Kato, H., Saito, M., Nagahata, Y., and Katayama, Y.: Degradation of ambient carbonyl

465        sulfide by Mycobacterium spp. in soil, Microbiology+. 154, 249-255, 2008.

466    Kesselmeier, J., Teusch, N., and Kuhn, U.: Controlling variables for the uptake of

467        atmospheric carbonyl sulfide by soil, J. Geophys. Res.: Atmos., 104, 11577-11584,

468        1999.

469    Kitz, F., Gerdel, K., Hammerle, A., Laterza, T., Spielmann, F. M., and Wohlfahrt, G.: In

470        situ soil COS exchange of a temperate mountain grassland under simulated

471        drought, Oecologia, 183, 851-860, 2017.

472    Kowalski, A. S., and Sánchezcañete, E. P.: A New Definition of the Virtual Temperature,

473        Valid for the Atmosphere and the $CO_2$-Rich Air of the Vadose Zone, J. Appl.

474        Meteorol. Clim., 49, 1238-1242, 2010.

475    Kuhn, U., Ammann, C., Wolf, A., Meixner, F., Andreae, M., and Kesselmeier, J.:

476        Carbonyl sulfide exchange on an ecosystem scale: Soil represents a dominant sink

477        for atmospheric COS, Atmos. Environ., 33, 995-1008, 1999.

478    Li, X., Liu, J., and Yang, J.: Variation of $H_2S$ and COS emission fluxes from
479        Calamagrostis angustifolia Wetlands in Sanjiang Plain, Northeast China, Atmos.
480        Environ., 40, 6303-6312, 2006.

481    Li, X. S., Sato, T., Ooiwa, Y., Kusumi, A., Gu, J. D., and Katayama, Y.: Oxidation of
482        elemental sulfur by Fusarium solani strain THIF01 harboring endobacterium
483        Bradyrhizobium sp, Microb. Ecol., 60, 96-104, 2010.

484    Liu, J., Geng, C., Mu, Y., Zhang, Y., Xu, Z., and Wu, H.: Exchange of carbonyl sulfide
485        (COS) between the atmosphere and various soils in China, Biogeosciences, 7, 753-
486        762, 2010.

487    Masaki, Y., Ozawa, R., Kageyama, K., and Katayama, Y.: Degradation and emission of
488        carbonyl sulfide, an atmospheric trace gas, by fungi isolated from forest soil,
489        FEMS Microbiol. Lett., 363, fnw197, 2016.

490    Maseyk, K., Berry, J. A., Billesbach, D., Campbell, J. E., Torn, M. S., Zahniser, M., and
491        Seibt, U.: Sources and sinks of carbonyl sulfide in an agricultural field in the
492        Southern Great Plains, P. Natl. Acad. Sci. U.S.A., 111, 9064-9069, 2014.

493    Ogée, J., Sauze, J., Kesselmeier, J., Genty, B., Van Diest, H., Launois, T., and Wingate,
494        L.: A new mechanistic framework to predict OCS fluxes from soils,
495        Biogeosciences, 13, 2221-2240, 2016.

496    Penman, H. L.: Gas and Vapor Movements in the Soli: I. The diffusion of vapors
497        through porous solids, J. Agric. Sci., 30, 437-462, 1940.

498    Piazzetta, P., Marino, T., and Russo, N.: The working mechanism of the beta-carbonic
499        anhydrase degrading carbonyl sulphide (COSase): a theoretical study, Phys. Chem.
500        Chem. Phys., 17, 14843-14848, 2015.

501    Sánchez-Cañete, E. P., Scott, R. L., Van Haren, J., and Barron-Gafford, G. A.:
502        Improving the accuracy of the gradient method for determining soil carbon dioxide
503        efflux, J. Geophys. Res.:Biogeo., 122, 2017.

504    Seibt, U., Kesselmeier, J., Sandoval-Soto, L., Kuhn, U., and Berry, J.: A kinetic analysis
505        of leaf uptake of COS and its relation to transpiration, photosynthesis and carbon
506        isotope fractionation, Biogeosciences, 7, 333-341, 2010.

507    Seibt, U., Wingate, L., Lloyd, J., and Berry, J. A.: Diurnally variable $\delta^{18}O$ signatures of

Atmospheric
Chemistry
and Physics
Discussions

Open Access

EGU

508       soil $CO_2$ fluxes indicate carbonic anhydrase activity in a forest soil, J. Geophys.

509       Res.: Atmos., 111, G04005, 2006.

510   Singer, A.: The soils of Israel, Springer Science & Business Media, 2007.

511   Smith, N. A., and Kelly, D. P.: Oxidation of carbon disulphide as the sole source of

512       energy for the autotrophic growth of Thiobacillus thioparus strain TK-m,

513       Microbiology+. 134, 3041-3048, 1988.

514   Steinbacher, M., Bingemer, H. G., and Schmidt, U.: Measurements of the exchange of

515       carbonyl sulfide (OCS) and carbon disulfide ($CS_2$) between soil and atmosphere

516       in a spruce forest in central Germany, Atmos. Environ., 38, 6043-6052, 2004.

517   Sun, W., Maseyk, K., Lett, C., and Seibt, U.: A soil diffusion–reaction model for surface

518       COS flux: COSSM v1, Geosci. Model. Dev., 8, 3055-3070, 2015.

519   Sun, W., Kooijmans, L. M. J., Maseyk, K., Chen, H., Mammarella, I., Vesala, T., Levula,

520       J., Keskinen, H., and Seibt, U.: Soil fluxes of carbonyl sulfide (COS), carbon

521       monoxide, and carbon dioxide in a boreal forest in southern Finland, Atmos. Chem.

522       Phys., 18, 1363-1378, 2018.

523   Svoronos, P. D., and Bruno, T. J.: Carbonyl sulfide: a review of its chemistry and

524       properties, Ind. Eng. Chem. Res., 41, 5321-5336, 2002.

525   Van Diest, H., and Kesselmeier, J.: Soil atmosphere exchange of carbonyl sulfide (COS)

526       regulated by diffusivity depending on water-filled pore space, Biogeosciences, 5,

527       475-483, 2008.

528   Viktor, A., and Cramer, M. D.: The influence of root assimilated inorganic carbon on

529       nitrogen acquisition/assimilation and carbon partitioning, New Phytol., 165, 157-

530       169, 2005.

531   Wehr, R., Commane, R., Munger, J. W., McManus, J. B., Nelson, D. D., Zahniser, M.

532       S., Saleska, S. R., and Wofsy, S. C.: Dynamics of canopy stomatal conductance,

533       transpiration, and evaporation in a temperate deciduous forest, validated by

534       carbonyl sulfide uptake, Biogeosciences, 14, 389, 2017.

535   Whelan, M. E., Min, D.-H., and Rhew, R. C.: Salt marsh vegetation as a carbonyl sulfide

536       (COS) source to the atmosphere, Atmos. Environ., 73, 131-137, 2013.

537   Whelan, M. E., and Rhew, R. C.: Carbonyl sulfide produced by abiotic thermal and

538    photodegradation of soil organic matter from wheat field substrate, J. Geophys.

539    Res.:Biogeo., 120, 54-62, 2015.

540    Whelan, M. E., Hilton, T. W., Berry, J. A., Berkelhammer, M., Desai, A. R., and

541    Campbell, J. E.: Carbonyl sulfide exchange in soils for better estimates of

542    ecosystem carbon uptake, Atmos. Chem. Phys., 16, 3711-3726, 2016.

543    Whelan, M. E., Lennartz, S. T., Gimeno, T. E., Wehr, R., Wohlfahrt, G., Wang, Y.,

544    Kooijmans, L. M. J., Hilton, T. W., Belviso, S., Peylin, P., Commane, R., Sun, W.,

545    Chen, H., Kuai, L., Mammarella, I., Maseyk, K., Berkelhammer, M., Li, K. F.,

546    Yakir, D., Zumkehr, A., Katayama, Y., Ogée, J., Spielmann, F. M., Kitz, F., Rastogi,

547    B., Kesselmeier, J., Marshall, J., Erkkilä, K. M., Wingate, L., Meredith, L. K., He,

548    W., Bunk, R., Launois, T., Vesala, T., Schmidt, J. A., Fichot, C. G., Seibt, U.,

549    Saleska, S., Saltzman, E. S., Montzka, S. A., Berry, J. A., and Campbell, J. E.:

550    Reviews and syntheses: Carbonyl sulfide as a multi-scale tracer for carbon and

551    water cycles, Biogeosciences, 15, 3625-3657, 2018.

552    White, M., Zhou, Y., Russo, R., Mao, H., Talbot, R., Varner, R., and Sive, B.: Carbonyl

553    sulfide exchange in a temperate loblolly pine forest grown under ambient and

554    elevated $CO_2$, Atmos. Chem. Phys., 10, 547-561, 2010.

555    Yang, F., Qubaja, R., Tatarinov, F., Rotenberg, E., and Yakir, D.: Assessing canopy

556    performance using carbonyl sulfide measurements, Glob. Change Biol., 24, 3486-

557    3498, 2018.

558    Yi, Z., Wang, X., Sheng, G., Zhang, D., Zhou, G., and Fu, J.: Soil uptake of carbonyl

559    sulfide in subtropical forests with different successional stages in south China, J.

560    Geophys. Res.: Atmos., 112, D08302, 2007.

Atmospheric
Chemistry
and Physics
Discussions

**Figure captions:**

**Figure 1.** Spatial variability of soil COS flux at three sites, between trees (a), between rows (b), and under tree (c). Each figure shows the diurnal cycling of soil COS flux in the four campaigns. Each data point was the hourly mean ± 1 S.E. (N=3).

**Figure 2.** Relationship of soil COS flux with soil moisture. Soil fluxes and mositure data point represent the diurnal average (N=24) of each microsite and season (i.e. each measurement campaign). Error bars represent ± 1 S.E. around the mean; errors for flux are about the size of the symbols.

**Figure 3.** Soil COS fluxes response to soil temperature linearly. Soil fluxes and represent the diurnal average (N=24) of each site and season (campaign), mositure data represent one sampling per day. Error bars represent ± 1 S.E. around the mean. The marked (black) data point were collected during irrigation campaign (enhanced uptake) and were excluded from the regression.

**Figure 4.** Mean COS and $CO_2$ concentrations at different soil depth. The COS concentration decreases exponentially with soil depth. The data point is the mean of the combined data at each of the four measurement campaigns (N=4; ± 1 S.E.).

**Figure 5.** Soil COS and $CO_2$ concentration profiles at the three microsites in four measurement campaigns. The data points are the mean of all measurements in a campaign (N=4, ± 1 S.E.)

**Figure 6.** The relationships between soil COS and $CO_2$ flux rates (chamber measurements; a). The response of soil relative uptake (SRU; normalized ratio of COS to $CO_2$ fluxes) to soil temperature (b) and to soil water content (c). The data points represent the diurnal average (N=24) of each site and season (measurement campaign). Error bars represent ± 1 S.E. around the mean (often the size of the symbol).

Atmospheric
Chemistry
and Physics
Discussions

Open Access

585 **Table 1.** Mean values of soil COS and $CO_2$ flux rates across sites (BR, between rows;

586 BT, between trees; UT, under tree), and seasons, together with the normalized ratio of

587 COS/$CO_2$ fluxes (SRU), and the mean soil temperature at 5 cm depth ($Ts$) and soil water

588 content (% by wt; $\theta$).

| Campaigns | Sites | COS flux (pmol m$^{-2}$ s$^{-1}$) | CO$_2$ flux (μmol m$^{-2}$ s$^{-1}$) | SRU | $Ts$ (ºC) | $\theta$ (%) |
|---|---|---|---|---|---|---|
| August, 2015 | BR | 1.83±0.08 | 0.77±0.04 | 1.85 | 31.66±1.01 | 9.98±0.28 |
| | BT | 0.06±0.05 | 3.33±0.05 | 0.01 | 29.09±0.20 | 19.77±0.02 |
| | UT | -3.64±0.13 | 10.79±0.12 | -0.26 | 28.80±0.26 | 24.03±0.40 |
| | | | | | | |
| December, 2015 | BR | -0.74±0.07 | 0.30±0.02 | -1.92 | 10.50±0.17 | 23.33±1.89 |
| | BT | -2.52±0.10 | 1.21±0.03 | -1.62 | 11.20±0.19 | 24.22±0.94 |
| | UT | -3.87±0.08 | 3.81±0.07 | -0.79 | 12.17±0.16 | 26.11±1.01 |
| | | | | | | |
| May, 2016 | BR | -0.77±0.02 | 0.32±0.02 | -1.88 | 21.67±0.32 | 15.56±0.38 |
| | BT | -0.05±0.04 | 1.31±0.05 | -0.03 | 22.20±0.34 | 15.70±1.03 |
| | UT | -1.80±0.11 | 10.78±0.54 | -0.13 | 20.35±0.38 | 22.11±1.44 |
| | | | | | | |
| July, 2016 | BR | 0.21±0.04 | 0.79±0.05 | 0.21 | 29.66±0.60 | 14.73±0.57 |
| | BT | 0.76±0.09 | 1.97±0.04 | 0.30 | 26.68±0.15 | 17.49±0.70 |
| | UT | -2.67±0.09 | 14.58±0.40 | -0.14 | 27.83±0.34 | 35.47±3.47 |

589

Atmospheric
Chemistry
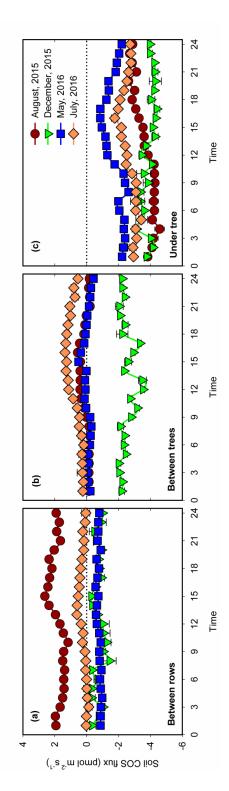and Physics
Discussions
Open Access

590

591

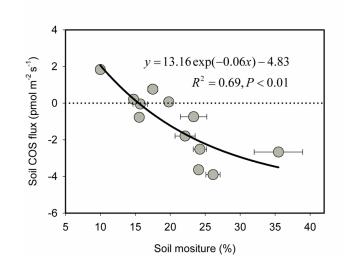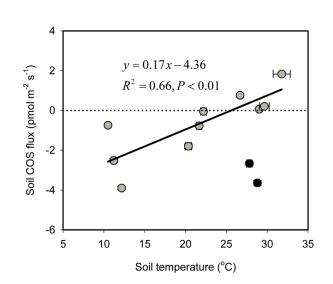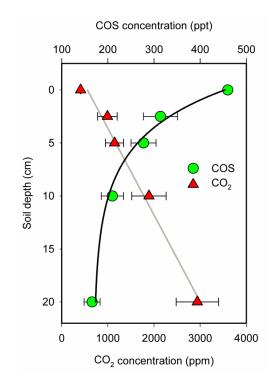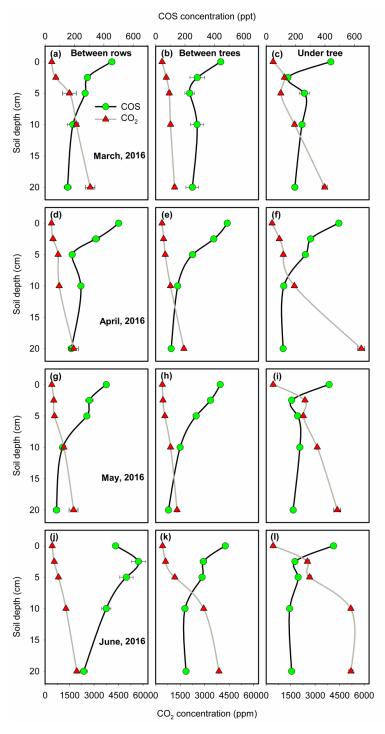**Table 2.** Estimates of soil COS and $CO_2$ fluxes from soil concentration gradient measurements ($T_s$, soil temperature; $\theta$, soil water content; BR, between rows; BT, between trees; UT, under tree.)

| Campaigns | Sites | COS flux (pmol m$^{-2}$ s$^{-1}$) | $CO_2$ flux (µmol m$^{-2}$ s$^{-1}$) | $CO_2$ diffusion coefficient (mm$^2$ s$^{-1}$) | COS diffusion coefficient (mm$^2$ s$^{-1}$) | $T_s$ (°C) | $\theta$ (%) |
|---|---|---|---|---|---|---|---|
| March, 2016 | BR | -1.31 | 2.34 | 5.21 | 4.40 | 17.9 | 19.4 |
| | BT | -1.15 | 2.21 | 4.80 | 4.05 | 16.2 | 21.8 |
| | UT | -2.10 | 5.89 | 4.76 | 4.02 | 17.3 | 22.4 |
| April, 2016 | BR | -1.55 | 1.07 | 6.66 | 5.62 | 23.0 | 11.0 |
| | BT | -0.89 | 1.14 | 6.44 | 5.43 | 20.4 | 11.6 |
| | UT | -1.74 | 4.73 | 6.01 | 5.07 | 22.4 | 15.2 |
| May, 2016 | BR | -0.98 | 2.21 | 5.68 | 4.79 | 21.9 | 17.4 |
| | BT | -0.51 | 1.24 | 5.06 | 4.27 | 22.0 | 21.6 |
| | UT | -1.20 | 11.36 | 3.11 | 2.63 | 20.1 | 34.5 |
| June, 2016 | BR | 1.55 | 2.63 | 6.61 | 5.57 | 35.9 | 15.5 |
| | BT | -1.17 | 2.60 | 5.20 | 4.39 | 26.3 | 21.7 |
| | UT | -1.19 | 11.85 | 3.02 | 2.55 | 22.9 | 35.6 |

592

**Figure 1**

**Figure 2**



$$y = 13.16\exp(-0.06x) - 4.83$$
$$R^2 = 0.69, P < 0.01$$

Atmospheric
Chemistry
and Physics
Discussions

**Figure 3**

**Figure 4**

**Figure 5**

**Figure 6**